

RESEARCH

Open Access



Diagnostic features of pediatric testicular yolk sac tumors: a 13-year retrospective analysis

Xiaoli Zheng^{1†}, Siqi Zhang^{2†}, Taiya Chen¹, Huan Zhang³, Shoulin Li⁴, Hongwu Zeng¹ and Wenhong Ye^{1*}

Abstract

Background Testicular yolk sac tumor (YST) is a rare neoplasm with limited practical guidance for preoperative diagnostic assessment. This study aims to conduct a retrospective analysis of the value of clinical profiles and MRI parameters in accurately diagnosing pediatric testicular YST while exploring characteristic indicators for these patients.

Methods This retrospective study analyzed eighty patients with a testicular mass who underwent surgical treatment and preoperative MRI. Clinical characters (age, preoperative serum alpha-fetoprotein (AFP) levels), and radiology features were recorded and compared. Subsequently, patients were categorized into YST and non-YST groups based on histology. Comparative statistical analyses were then used to compare factors between the two groups. The receiver operating characteristic curve (ROC) analysis was conducted to evaluate the diagnostic performance of the indicators for pediatric testicular YST.

Results Forty patients (50%) were diagnosed with YST. In comparison to the non-YST group, patients with testicular YST were younger and had larger tumor sizes, accompanied by significantly elevated AFP levels. On MRI, most YST cases ($n = 38$) exhibited predominantly solid lesions, whereas non-YST tumors were more likely to contain cystic components. The bright dot sign and thickened spermatic cord might also be helpful in differentiating YST ($p < 0.05$). The optimal factor for diagnosing testicular YST was signal intensity, with an AUC value of 0.936 (95%CI: 0.877 ~ 0.995).

Conclusions A predominantly solid testicular mass with a bright dot sign, thickened spermatic cord ipsilaterally, and elevated AFP levels should raise suspicion for YST.

Keywords Testicular tumor, Yolk sac tumor, Pediatrics, Magnetic resonance imaging, Diagnosis

Introduction

Yolk sac tumors (YST), also known as primitive endodermal tumors or endodermal sinus tumors, are aggressive malignant neoplasms originating from primitive germ cells. Although testicular YST has a low incidence rate of less than 1% [1], it accounts for 70–80% of prepubertal malignant testicular tumors and represents the most common form of childhood testicular cancer [2, 3]. YST has a significant mortality rate due to its high malignancy, subtle onset, and rapid progression [4, 5].

The management of testicular YST is heavily contingent upon the age of the patient [6], with 90% of prepubertal

[†]Xiaoli Zheng and Siqi Zhang contributed equally to this work.

*Correspondence:

Wenhong Ye
yewenhong21@163.com

¹Department of Radiology, Shenzhen Children's Hospital, 7019 Yitian Road, Futian District, Shenzhen 518038, China

²Department of Radiology and Nuclear Medicine, Xuanwu Hospital Capital Medical University, Beijing 100053, China

³Department of Pathology, Shenzhen Children's Hospital, 7019 Yitian Road, Futian District, Shenzhen 518038, China

⁴Department of Urology, Shenzhen Children's Hospital, 7019 Yitian Road, Futian District, Shenzhen 518038, China



© The Author(s) 2024. **Open Access** This article is licensed under a Creative Commons Attribution-NonCommercial-NoDerivatives 4.0 International License, which permits any non-commercial use, sharing, distribution and reproduction in any medium or format, as long as you give appropriate credit to the original author(s) and the source, provide a link to the Creative Commons licence, and indicate if you modified the licensed material. You do not have permission under this licence to share adapted material derived from this article or parts of it. The images or other third party material in this article are included in the article's Creative Commons licence, unless indicated otherwise in a credit line to the material. If material is not included in the article's Creative Commons licence and your intended use is not permitted by statutory regulation or exceeds the permitted use, you will need to obtain permission directly from the copyright holder. To view a copy of this licence, visit <http://creativecommons.org/licenses/by-nc-nd/4.0/>.

patients experiencing a favorable prognosis following surgical resection [7]. This underscores the critical importance of timely detection and intervention in determining the prognosis [8]. Additionally, the treatment approaches for benign and malignant testicular tumors differ significantly. In prepubertal patients, testis-sparing surgery, aimed at preserving testicular function, has become a widely accepted approach for benign testicular tumors, while malignant lesions are addressed through radical orchidectomy [9]. Therefore, ensuring an accurate preoperative diagnosis is of paramount importance.

Previous research on testicular YST has predominantly focused on analyzing clinical indicators, particularly prognostic risk factors [10, 11]. An elevated serum alpha-fetoprotein (AFP) level has long been considered a reliable marker for diagnosis and assessment [12]. Imaging plays a crucial role in managing testicular tumors in children and adolescents. However, due to the rarity of pediatric testicular tumors, there has been limited attention on radiological feature analysis, with only a few case reports available. Consequently, this study aims to retrospectively analyze the MRI features of pediatric testicular YST to enhance the accuracy of preoperative diagnosis, providing valuable insights for clinical decision-making on surgical options.

Materials and methods

Patient selection

We retrospectively reviewed patients undergoing surgical treatment for testicular mass at the XXX Hospital between January 2010 and December 2023. Patients were further selected matching the following criteria: (1) baseline clinical data were available and complete; (2) pelvic MRI examination was performed in children before the biopsy and treatment; (3) all patients were confirmed with pathological outcomes. Exclusion criteria were incomplete clinical data or unqualified preoperative MRI images. 80 children were finally included in this study, including 40 YSTs and 40 other tumors, approved by the local hospital's Ethics Committee (No. 2022021). Figure 1 shows the workflow for patient selection.

MRI acquisition

Four imaging sequences were selected for the preoperative pelvic MRI of each patient, namely, T1WI, CE-T1WI, T2WI, and T2-Dixon. The Siemens Skyra 3.0 T superconducting MR scanner was utilized with an 18-channel phased-array body coil. The specific parameters are as follows: T1WI adopts T1_tse_tra sequence: TR=560ms, TE=10-20ms, slice thickness=5 mm, slice spacing=5.5 mm; CE-T1WI adopts T1_vibe_dixon_tra/cor/sag+c sequence: TR=540ms, TE=10-20ms, slice thickness=5 mm, slice spacing=5.5 mm; T2WI adopts

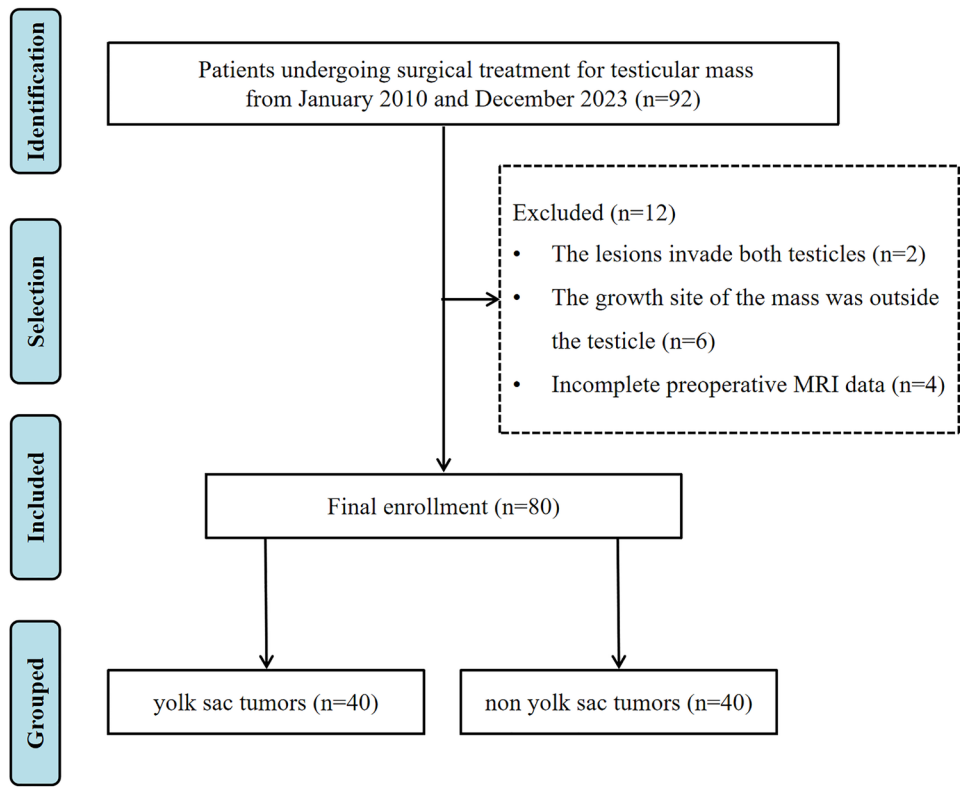


Fig. 1 Flowchart of patient selection

T2_tse_tra sequence: TR=4000-5000ms, TE=84-98ms, slice thickness=5 mm, slice spacing=5.5 mm; T2-Dixon adopts T2_tse_dixon_tra/cor/sag fat and water sequence: TR=2110ms, TE=65ms, slice thickness=4 mm, slice spacing=4.8 mm. Contrast agent GD-DTPA was used for enhanced scanning with a dose of 0.1 mmol/kg.

Clinical profiles

Baseline presurgical clinical profiles, laboratory tests, and pathologic data were collected from the medical records. The clinical factors considered included age, preoperative serum alpha-fetoprotein (AFP) levels, and histopathology. AFP and Glypican-3 examinations were used to confirm the subtypes of YST further. Subsequently, for the analysis, the patients were categorized into either the YST group or the non-YST group based on their histopathological outcomes.

Imaging review

Two radiologists specializing in pediatric oncology imaging retrospectively reviewed all images without knowing the patients' clinical histories, laboratory tests, and pathological outcomes. Image reviews were done independently and by consensus. When the two radiologists disagreed, a third radiologist with 25 years of experience provided the final opinion and facilitated consensus.

Each mass was assessed and characterized based on several MRI features: its location of growth, size (maximum diameter), shape (oval or irregular), signal intensity (predominantly solid, solid-cystic, or predominantly cystic), internal composition evaluated based on MRI signal (presence of hemorrhage, necrosis, calcification, or fatty tissue), degree of enhancement, and the presence of the

“bright dot” sign. Additionally, MRI findings for spermatic cord thickening and hydrocele were also evaluated.

Especially, the tumor size and the volume of the cystic component were measured using the longest diameter of the maximum multiplanar reformation section as the criterion. The signal intensity was subjectively assessed and categorized as predominantly solid, solid-cystic, and predominantly cystic, corresponding to the volume of cystic lesions less than 25%, between 25% and 75%, and greater than 75% of the tumor volume, respectively [13]. The level of enhancement was subjectively evaluated and grouped into the following categories [14]: mild, when the enhancement was like that of adjacent muscle; moderate, when the enhancement was higher than that of muscle but lower than that of blood vessels; and marked, when the enhancement was approaching that of blood vessels. The “bright dot” sign was defined as the different number of dilated vessels in the tumor on post-contrast images [15]. The typical MRI characteristics of the YST and teratoma are exemplified in Figs. 2 and 3.

Statistical analysis

SPSS 18.0 (IBM, New York, USA) statistical analysis software was used for data analysis. Normally distributed data were expressed as mean \pm standard deviation ($\bar{x} \pm SD$), while non-normally distributed data were expressed as a median and interquartile range. The independent sample t-test or the Mann-Whitney U test was used to analyze continuous variables, and the chi-square or Fisher's exact test was for categorical variables. A *p*-value of <0.05 was considered to be statistically significant. The regression models were used to assess each factor's diagnostic efficacy, and the receiver operating

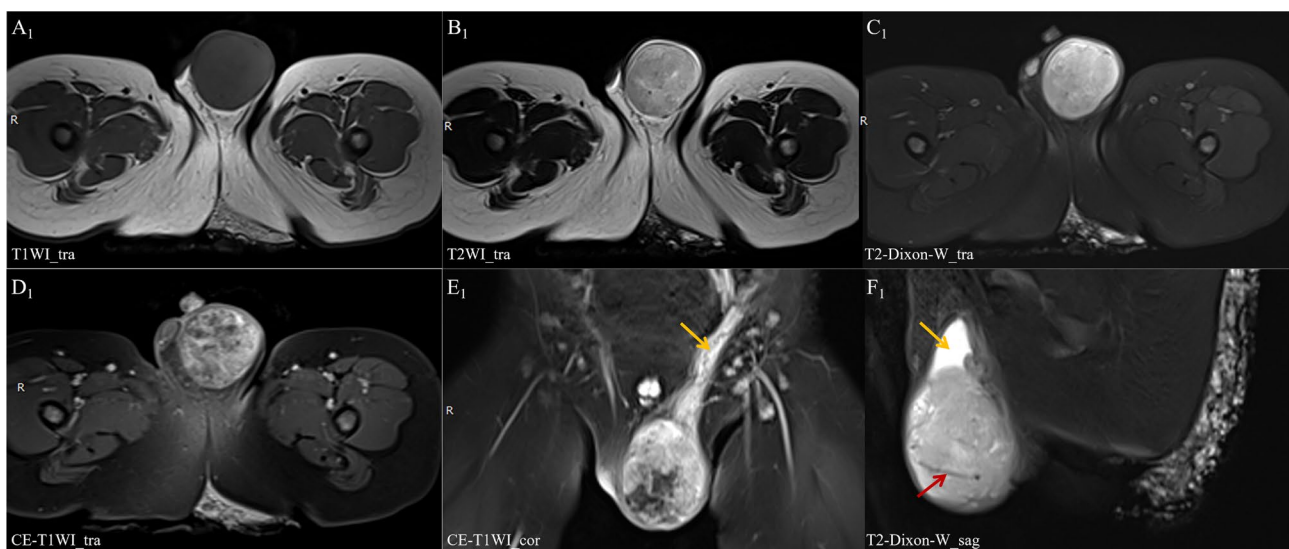


Fig. 2 The example of testicular yolk sac tumor: images of a 17-months-old male patient treated by radical orchidectomy. The lesion located in the left scrotum showed as a predominantly solid mass with significant enhancement. The yellow arrow on figure (E₁) indicates thickened spermatic cord on the same side. Hydrocele (yellow arrow) and bright dot sign (red arrow) can be seen on figure (F₁)

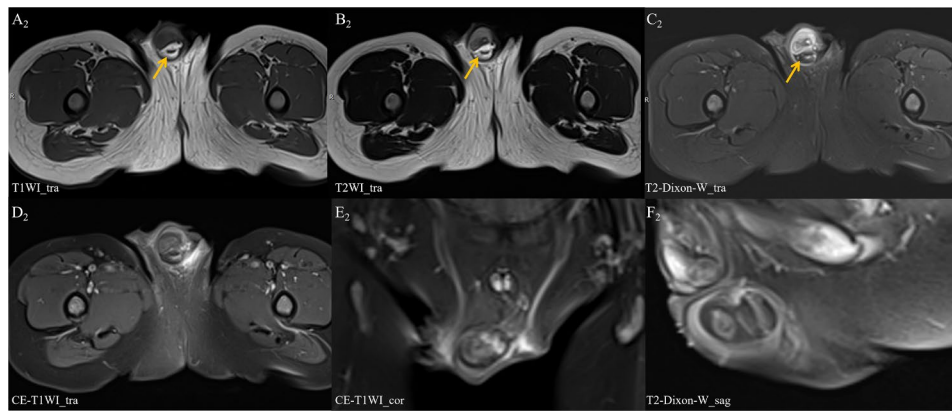


Fig. 3 The example of testicular teratoma: images of a 29-months-old male patient treated by testis-sparing surgery. The lesion located in the left scrotum appears as a solid cystic mass with fat components (depicted by the yellow arrow)

characteristic (ROC) curve was plotted. The area under the curve (AUC) with a 95% confidence interval was calculated, and diagnostic performance, including sensitivity and specificity, was determined at the optimal cut-off value.

Results

Clinical findings

A total of 80 patients were included, of which 40 (50.0%) were confirmed as YST. As the 4th edition of the WHO Testicular Tumor Classification (2016) was the first to categorize YST into prepubertal and postpubertal types, 23 of the 40 patients in our study, diagnosed after 2016, were classified as prepubertal-type YST. The non-YST datasets were comprised of teratomas ($n=34$), embryonal cell carcinomas ($n=2$), and sex cord-stroma tumors ($n=4$). Patients diagnosed with YST were younger than those in the non-YST group (mean age of 1.47 vs. 4.68 years, $p<0.05$). The serum level of AFP in the YST group was much higher than in the other group (mean value of 4403.43 vs. 24.24 ng/ml, $p<0.05$), while the average tumor size was larger (mean size of 29.95 vs. 18.70 mm, $p<0.05$).

The proportion of patients undergoing testis-sparing surgery (TSS) was 1/40 in the YST group and 37/40 in the non-YST group. The only YST patient who underwent TSS did so at the strong request of the family, as the patient was only 11 months old. In the non-YST group, three patients underwent radical orchiectomy (RO). One required RO due to the large size of the mass, which made it difficult to preserve normal testicular tissue; pathology confirmed an immature teratoma. The other two patients required secondary RO due to recurrence or malignant transformation of the lesion. Postoperative pathology identified one mature teratoma and one immature teratoma in these cases.

Follow-up data showed favorable outcomes in 32 of the 36 patients in the YST group, with no recurrence or

metastasis, including the patients who underwent TSS. Four patients had poor outcomes: metastasis occurred within six months in three cases (one to the lungs and two to the lymph nodes), and one patient had a significant rise in serum AFP levels one year after surgery, despite negative imaging results. All 40 patients in the non-YST group had favorable recoveries.

Radiological features

Among the YST patients, 21 cases were in the left testicle. Compared to the non-YST group, all the masses in the YST datasets exhibited an oval shape. Regarding signal intensity, YST typically displayed a predominance of solid components with significant enhancement, while non-YST tumors tended to have a higher proportion of cystic components, resulting in mild enhancement. The bright dot sign, a frequently observed feature in germ cell tumors, could also serve as an important diagnostic indicator for YST, being present in 23 (57.5%) of the YST patients in our cohort. Necrosis is commonly observed in YST, whereas calcification and fat deposition are exclusively seen in non-YST entities. A thickened spermatic cord was detected in 38 (95.0%) YST patients, followed by hydrocele, which was detected in 31 (77.5%) YST patients. The details are shown in Table 1.

Key diagnostic indicators

Stepwise regression results showed that size ($\beta=0.006$, 95%CI: -0.011~-0.001, $p=0.013$), signal intensity ($\beta=0.362$, 95%CI: -0.439~-0.286, $p=0.000$), fat ($\beta=-0.383$, 95%CI: 0.241~0.526, $p=0.000$), bright-dot sign ($\beta=0.168$, 95%CI: -0.299~-0.037, $p=0.014$), and thickened spermatic cord ($\beta=0.135$, 95%CI: -0.264~-0.007, $p=0.043$) were independent influencing factor for YST diagnostics. The ROC curves were employed to assess the diagnostic efficacy of clinical and MRI indicators in pediatric YST patients. The cut-off value of the tumor size was 26 mm (AUC=0.805, 95%CI: 0.711~0.900,

Table 1 Comparison of clinical and radiological data between the YST and non-YST cohorts

Factors	YST (n = 40)	non-YST (n = 40)	p -Value
Age (year) ^a	1.47 ± 1.05	4.68 ± 4.01	0.000
AFP (ng/ml) ^a	4403.43 ± 6588.70	24.24 ± 82.67	0.000
Size (mm) ^a	29.95 ± 11.41	18.70 ± 8.37	0.000
Location n (%) ^b			0.653
Left	21 (53.5)	23 (57.5)	
Right	19 (47.5)	17 (42.5)	
Shape n (%) ^b			0.001
Oval	40 (100)	31 (77.5)	
Irregular	0 (0)	9 (22.5)	
Signal intensity n (%) ^b			0.000
Predominantly solid	38 (95)	4 (10)	
Solid-cystic	2 (5)	20 (50)	
Predominantly cystic	0 (0)	16 (40)	
Calcification n (%) ^b	0 (0)	12 (30)	0.000
Fat n (%) ^b	0 (0)	13 (32.5)	0.000
Hemorrhage n (%) ^b	1 (2.5)	1 (2.5)	1.000
Necrosis n (%) ^b	28 (70)	14 (35)	0.002
Enhance degree n (%) ^b			0.000
Mild	0 (0)	20 (50)	
Moderate	0 (0)	9 (22.5)	
Marked	40 (100)	11 (27.5)	
Bright-dot sign n (%) ^b	23 (57.5)	0 (0)	0.000
Thickened spermatic cord n (%) ^b	38 (95)	13 (32.5)	0.000
Hydrocele n (%) ^b	31 (77.5)	11 (27.5)	0.000

a. Data are mean, with standard deviation. The independent sample t-test was used to analyze

b. Data are numbers of patients with percentages in parentheses. The chi-square or Fisher's exact test was used to analyze

sensitivity=0.65, specificity=0.83). The diagnostic performance of the signal intensity stands out as the most optimal among the five features. The AUC value of the signal intensity, fat, bright-dot sign, and thickened spermatic cord in the diagnosis of YST was 0.936 (95%CI: 0.877 ~ 0.995, sensitivity=0.90, specificity=0.95), 0.663 (95%CI: 0.542 ~ 0.783, sensitivity=0.33, specificity=1.00), 0.788 (95%CI: 0.683 ~ 0.892, sensitivity=1.00, specificity=0.58), 0.813 (95%CI: 0.713 ~ 0.912, sensitivity=0.68, specificity=0.95), respectively. The visualization of the ROC curve results is shown in Fig. 4.

Discussion

Yolk sac tumor (YST) is the most common primary tumor of the testes in prepubertal patients [16]. Its pathological features include reticular-microcystic, endodermal sinus (Schiller-Duval bodies), glandular, papillary, and solid patterns [17, 18]. Research [19, 20] indicates that YST in prepubertal patients consistently demonstrates indolent behavior, leading to a favorable prognosis. Therefore, timely and accurate diagnosis is crucial in enhancing postoperative recovery and improving the quality of life in affected children. When evaluating testicular pathology in children, ultrasonography (US) and MRI are the primary imaging modalities [9]. MRI has gained preference due to its excellent soft tissue

resolution and the availability of gadolinium contrast agents. As a result, understanding the key clinical and MRI findings related to diagnosis is significant for personalized preoperative diagnosis and treatment evaluation, and for improving postoperative quality of life in children with testicular YST.

The statistical results of clinical data showed that patients diagnosed with YST were even younger, with a mean age of 1.5 years, consistent with the epidemiological survey result that the median age for the presentation of YST is 16 months [21]. Testicular YSTs often secrete elevated levels of AFP, making it a key biomarker for both diagnosis and monitoring [22]. However, it is important to note that the diagnostic value of AFP may be influenced by natural increases in infants under 12 months of age. Zhou et al. [23] reported that while AFP levels in testicular teratomas in patients under 1 year may show physiological increases, they typically remain below 100 ng/ml, which is consistent with our findings. In contrast, AFP levels in YSTs are significantly elevated, with previous studies showing that over 90% of YSTs are associated with raised AFP levels [24]. Our study similarly confirms the substantial diagnostic utility of AFP in YST.

Our study has revealed a correlation between larger tumor diameter and testicles YST. Under general oncological principles, malignant tumors typically exhibit a

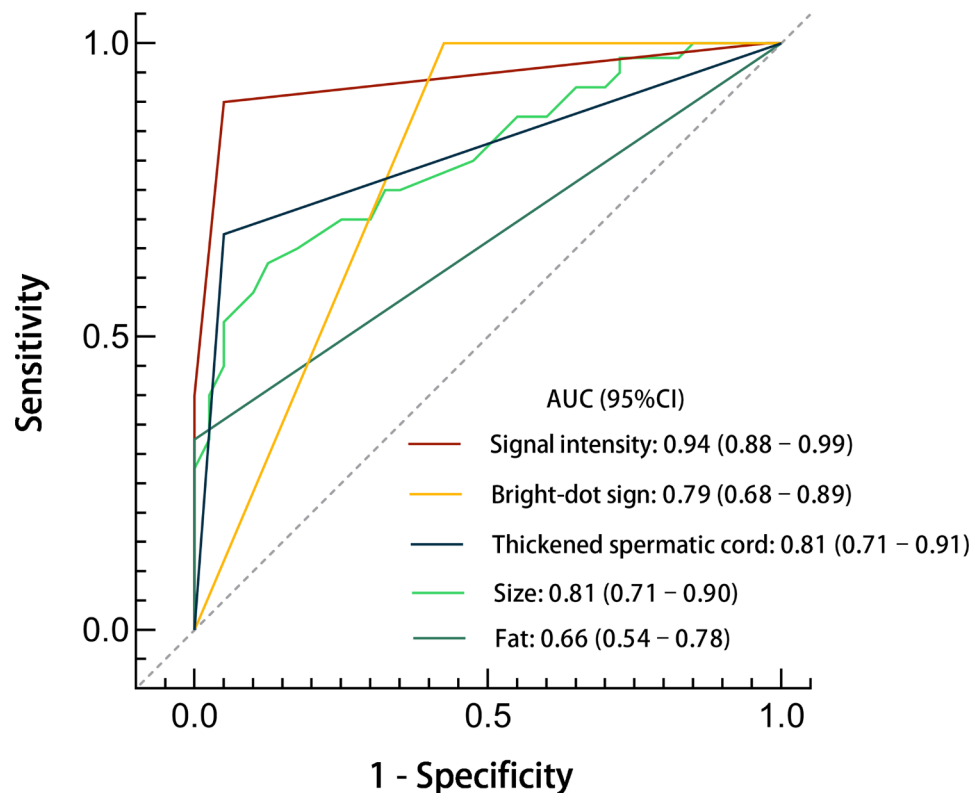


Fig. 4 Comparing the predictive performance of various indicators

faster growth rate than benign tumors, underscoring the association between tumor diameter and malignancy. Currently, there is no universally accepted criterion for tumor diameter due to the low prevalence of testicular tumors, making it challenging to differentiate between benign and malignant cases reliably. Previous research by Shilo et al. [25] reported that using a size cutoff of 18.5 mm, 38.5% of smaller lesions were found to be benign, whereas only 2% of lesions above this threshold were benign. Moreover, Song et al. [11] used logistic regression analysis to confirm that an increase in tumor diameter corresponds to a higher risk of malignancy. Consistent with these findings, our study observed that the average tumor size of YST exceeded that of non-YST cases. Moreover, as tumors enlarge, they apply pressure on nearby tissue structures, resulting in the ipsilateral spermatic vein thickening, which can be directly identified and evaluated on MRI. This further strengthens the correlation between the size of the tumor and malignancy.

In this cohort, YSTs primarily present as solid masses with small cystic components, whereas non-YST tumors (primarily teratomas) are characterized by mixed masses with scattered fat and calcifications. The MRI signal intensity characteristics play a crucial role in differentiating between these tumor types, demonstrating an AUC of 0.94. Additionally, micro cysts within YST masses

correspond to histological features of loose reticular cells [26], while the bright dot sign in YST is thought to result from the tumor's release of angiogenic factors, which stimulate vascular proliferation [27]. This results in rich blood flow within and around the tumor, manifesting as a branching pattern on MRI. On the other hand, MRI fat signals aid in the differential diagnosis of teratomas, which originate from three germ layers and possess a rich internal structure [28]. Therefore, these distinctive MRI features serve as crucial diagnostic indicators for discriminating between YST and non-YST tumors, with each presenting unique radiological characteristics that highlight their pathological nature.

This study has several potential limitations. First, it has limitations inherent to the retrospective study design and manual measurement. Second, the YST dataset includes only the prepubertal subtype, which may limit the interpretation. Finally, some data were incomplete due to the lengthy period involved, and DWI sequence analysis, which is useful in diagnosing testicular masses, was not included. These issues need to be further explored in the future.

In conclusion, specific MRI signs can enhance the accuracy of imaging diagnosis and differentiation of pediatric testicular YST. A predominantly solid testicular mass, accompanied by the bright dot sign, ipsilateral thickened

spermatic cord, and elevated AFP levels, should strongly suggest the possibility of YST.

Acknowledgements

Not applicable.

Author contributions

Xiaoli Zheng and Siqi Zhang contributed equally to this work. Xiaoli Zheng and Siqi Zhang conceived the paper and prepared the manuscript. Xiaoli Zheng and Taiya Chen performed MRI examinations and analyzed data. Huan Zhang and Shoulin Li collected clinical data of patients. Siqi Zhang wrote and edited the manuscript. Hongwu Zeng and Wenhong Ye revised the manuscript.

Funding

This work was supported by the Sanming Project of Medicine in Shenzhen (SZSM202011005) from Shenzhen Medical and Health Project and the Guangdong High-level Hospital Construction Fund (ynkt2021-zz47).

Data availability

The data that support the findings of this study are available from the corresponding author upon reasonable request.

Declarations

Ethics approval and consent to participate

Ethical approval: The studies involving human participants were reviewed and approved by the Medical Ethics Committee of the local hospital (No. 2022021).

Consent to participate

All the participants and guardians of adolescents signed a written informed consent form after receiving a complete study description.

Competing interests

The authors declare no competing interests.

Received: 3 September 2024 / Accepted: 1 December 2024

Published online: 05 December 2024

References

- Gilligan T, Lin DW, Aggarwal R, et al. Testicular Cancer, Version 2.2020, NCCN Clinical Practice guidelines in Oncology. *J Natl Compr Canc Netw* Dec. 2019;17(12):1529–54. <https://doi.org/10.6004/jnccn.2019.0058>.
- Fonseca A, Frazier AL, Shaikh F. Germ cell tumors in adolescents and young adults. *J Oncol Pract*. 2019;15(8):433–41.
- Liu P, Li W, Song HC, Jiao LL, Zhang WP, Sun N. Characteristics, treatment decisions and outcomes of prepubertal testicular germ cell tumor: a descriptive analysis from a large Chinese center. *J Pediatr Urol* Oct. 2018;14(5):e4431–7. <https://doi.org/10.1016/j.jpuro.2018.02.030>.
- Jarvis H, Cost NG, Saltzman AF. Testicular tumors in the pediatric patient. Elsevier; 2021. p. 151079.
- Stein R, Quaedackers J, Bhat NR, et al. EAU-ESPU pediatric urology guidelines on testicular tumors in prepubertal boys. *J Pediatr Urol* Aug. 2021;17(4):529–33. <https://doi.org/10.1016/j.jpuro.2021.06.006>.
- Wei Y, Wu S, Lin T, et al. Testicular yolk sac tumors in children: a review of 61 patients over 19 years. *World J Surg Oncol*. 2014;12:1–9.
- Maizlin II, Dellinger M, Gow KW, et al. Testicular tumors in prepubescent patients. *J Pediatr Surg* Sep. 2018;53(9):1748–52. <https://doi.org/10.1016/j.jpedsurg.2017.09.020>.
- Chiu CC, Jaing TH, Lai JY, et al. Malignant testicular tumors in children: a single institution's 12-year experience. *Med (Baltimore)* Jul. 2022;22(29):e29735. <https://doi.org/10.1097/MD.00000000000029735>.
- Hermann AL, L'Hermine-Coulomb A, Irtan S, et al. Imaging of Pediatric Testicular and Para-testicular tumors: a Pictorial Review. *Cancers (Basel)* Jun. 2022;29(13). <https://doi.org/10.3390/cancers14133180>.
- Li M, Wang J, Li J, et al. Develop and validate nomogram to predict cancer-specific survival for patients with testicular yolk sac tumors. *Front Public Health*. 2022;10:1038502. <https://doi.org/10.3389/fpubh.2022.1038502>.
- Song G, Xiong GY, Fan Y, et al. The role of tumor size, ultrasonographic findings, and serum tumor markers in predicting the likelihood of malignant testicular histology. *Asian J Androl* Mar-Apr. 2019;21(2):196–200. https://doi.org/10.4103/aja.aja_119_18.
- O'Neill AF, Xia C, Krailo MD, et al. Alpha-fetoprotein as a predictor of outcome for children with germ cell tumors: a report from the malignant germ cell International Consortium. *Cancer* Oct. 2019;15(20):3649–56. <https://doi.org/10.1002/cncr.32363>.
- Li YK, Zheng Y, Lin JB, et al. CT imaging of ovarian yolk sac tumor with emphasis on differential diagnosis. *Sci Rep* Jun. 2015;15(5):11000. <https://doi.org/10.1038/srep11000>.
- Sun F, Zhao SH, Li HM, Bao L, Xu L, Wang DB. Computed tomography and magnetic resonance imaging appearances of malignant vaginal tumors in children: endodermal sinus tumor and Rhabdomyosarcoma. *J Comput Assist Tomogr* Mar/Apr. 2020;44(2):193–6. <https://doi.org/10.1097/RCT.0000000000000954>.
- Shaban AM, Rezvani M, Elsayes KM, et al. Ovarian malignant germ cell tumors: cellular classification and clinical and imaging features. *Radiographics*. 2014;34(3):777–801.
- Kusler KA, Poynter JN. International testicular cancer incidence rates in children, adolescents and young adults. *Cancer Epidemiol* Oct. 2018;56:106–11. <https://doi.org/10.1016/j.canep.2018.08.002>.
- Young RH. The yolk sac tumor: reflections on a remarkable neoplasm and two of the many intrigued by it—Gunnar Teilum and Aleksander Tølerman—and the bond it formed between them. *Int J Surg Pathol*. 2014;22(8):677–87.
- Liu X, Feng S, Zhao L, Luo L. Clinical characteristics and prognostic models of gonadal and extra-gonadal yolk sac tumors: a population-based analysis in children and adolescents. *World J Urol* Nov. 2023;41(11):3009–17. <https://doi.org/10.1007/s00345-023-04616-4>.
- Cost NG, Lubahn JD, Adibi M, et al. A comparison of pediatric, adolescent, and adult testicular germ cell malignancy. *Pediatr Blood Cancer* Mar. 2014;61(3):446–51. <https://doi.org/10.1002/pbc.24773>.
- Zhao Q, Li M, Sun Q, et al. Clinical characteristics of malignant germ cell tumors in adolescents: a multicenter 10-year retrospective study in Beijing. *Cancer Innov* Dec. 2023;2(6):524–31. <https://doi.org/10.1002/cai2.87>.
- de Campos Vieira Abib S, Chui CH, Cox S, et al. International Society of Paediatric Surgical Oncology (IPSO) Surgical Practice guidelines. *Ecanermedicallscience*. 2022;16:1356. <https://doi.org/10.3332/ecancer.2022.1356>.
- Radford A, Peycelon M, Haid B, Powis M, Lakshminarayanan B. Testicular-sparing surgery in the pediatric population: Multicenter review of practice with review of the literature. *Curr Opin Urol*. 2019;29(5):481–6.
- Zhou G, Sun F, Yu X, et al. Clinical characteristics and long-term management of prepubertal testicular teratomas: a retrospective, multicenter study. *Eur J Pediatr* Apr. 2023;182(4):1823–8. <https://doi.org/10.1007/s00431-023-04859-8>.
- Patel P, Balise R, Srinivas S. Variations in normal serum alpha-fetoprotein (AFP) levels in patients with testicular cancer on surveillance. *Onkologie*. 2012;35(10):588–91. <https://doi.org/10.1159/000342695>.
- Shilo Y, Zisman A, Lindner A, et al. The predominance of benign histology in small testicular masses. *Urol Oncol* Sep. 2012;30(5):719–22. <https://doi.org/10.1016/j.urolonc.2010.08.022>.
- Sanguesa C, Veiga D, Llavorador M, Serrano A. Testicular tumours in children: an approach to diagnosis and management with pathologic correlation. *Insights Imaging* May. 2020;27(1):74. <https://doi.org/10.1186/s13244-020-00867-6>.
- Cornejo KM, Frazier L, Lee RS, Kozakewich HP, Young RH. Yolk sac tumor of the Testis in infants and children. *Am J Surg Pathol*. 2015;39(8):1121–31.
- Chang MY, Shin HJ, Kim HG, Kim MJ, Lee MJ. Prepubertal testicular teratomas and epidermoid cysts: comparison of clinical and Sonographic features. *J Ultrasound Med* Oct. 2015;34(10):1745–51. <https://doi.org/10.7863/ultra.15.14.09032>.

Publisher's note

Springer Nature remains neutral with regard to jurisdictional claims in published maps and institutional affiliations.